On the Electrochemically Grown Quasi-One-Dimensional $KCu_{7-x}S_4$ Series ($0 \leq x \leq 0.34$): Nonstoichiometry, Superlattice, and Unusual Phase Transitions

He Li,[†] Richard Mackay,[†] Shiou-Jyh Hwu,*[,†] Yung-Kang Kuo,[‡] Malcolm J. Skove,[‡] Yasuhiro Yokota,[§] and Tsukio Ohtani[§]

Department of Chemistry and Materials Science & Engineering Program, Clemson University, Clemson, South Carolina 29634-1905, Department of Physics and Astronomy, Clemson University, Clemson, South Carolina 29634-1911, and Research Institute of National Sciences and Laboratory for Solid State Chemistry, Okayama University of Science, Ridai-cho 1-1, Okayama 700-0005, Japan

Received April 1, 1998. Revised Manuscript Received June 29, 1998

Whiskers of the quasi-one-dimensional copper(I) sulfide series $KCu_{7-x}S_4$ ($0 \leq x \leq 0.34$) were grown by employing electrochemical (E-Chem) methods via anodic dissolution of copper electrodes. The compound series can be prepared at 110 °C in ethylenediamine solution of polysulfide K_2S_n ($n = 5, 6$) electrolytes and, in some cases, CuCl. Single-crystal structure analysis has reconfirmed the once ambiguous space group issue, and the study has also revealed that the KCu_7S_4 phase reported by Ohtani et al. is nonstoichiometric. The present investigations on as-grown whiskers show that the previously observed unusual insulator-to-metal transition can be reproduced by the $KCu_{6.86}S_4$ phase. At room temperature, $KCu_{6.66(4)}S_4$ crystallizes in the tetragonal space group $I4/m$ (No. 87) with $a = 10.179(2)$ Å, $c = 3.790(2)$ Å, $V = 392.7(2)$ Å^3, and $Z = 2$; $KCu_{6.82(3)}S_4$ in $I4/m$ (No. 87) with $a = 10.177(2)$ Å, $c = 3.822(2)$ Å, $V = 395.8(2)$ Å^3, and $Z = 2$; $KCu_{7.00(2)}S_4$ in $P4/n$ (No. 85) with $a = 10.177(2)$ Å, $c = 7.722(2)$ Å, $V = 799.8(3)$ Å^3, and $Z = 4$. Refined cell volumes increase linearly with increasing copper content. The extended framework resembles the $(NH_4)Cu_7S_4$ structure. It consists of quasi-one-dimensional Cu_4S_4 columns interlinked by tetrahedral copper chains. New evidence shows that the title series exhibits complicated structure patterns with regard to the ordering of the Cu^+ cation along the tetrahedral chain. The nonstoichiometry and cation ordering are likely responsible for the anomalies observed in transport properties (*Phys. Rev. B.* **1998**, *57*, 3315−3325). A self-consistent model with respect to local ordering is discussed, and a recently proposed diffusive one-dimensional ordering model at the transitions is reiterated. The detailed synthesis and structure, along with preliminary electron diffraction studies and temperature-dependent magnetic susceptibility measurements, of the title series are presented.

Introduction

The ternary A−Cu−S system (A = monovalent cation) presents a rich structural chemistry that merits intensive experimental and theoretical studies of transport phenomena of low-dimensional solids.[1−10] In the potassium (A = K) copper(I) sulfide system, not counting polysulfides, the known phases include KCuS,[2] KCu_4S_3,[3−6] $K_3Cu_8S_6$,[3,7] KCu_3S_2,[8] and KCu_7S_4.[9,10] All of these phases, except KCu_7S_4, are structurally well-characterized by single-crystal X-ray diffraction methods. The KCuS structure consists of one-dimensional Cu−S chains while KCu_4S_3, $K_3Cu_8S_6$, and KCu_3S_2 exhibit two-dimensional Cu−S layers. The KCu_7S_4 lattice is composed of a three-dimensional Cu−S framework which contains pseudo-one-dimensional channels in which the K^+ cations reside (see later discussion).

Three compounds, $K_3Cu_8S_6$, KCu_3S_2, and KCu_7S_4, show an interesting structural correlation (Figure 1). Each contains Cu_4S_4 columns, where the copper in the column is three-coordinate with respect to sulfur atoms. To reflect upon the content of the unit structure, the formulas can be rewritten as $K_3Cu_4S_2[Cu_4S_4]$, K_2Cu_2-

[†] Department of Chemistry and Materials Science & Engineering Program, Clemson University.
[‡] Department of Physics and Astronomy, Clemson University.
[§] Okayama University of Science.

(1) (a) Eichhorn, B. W. In *Ternary Transition-Metal Sulfides*; K. D. Karlin, Ed.; *Progress in Inorganic Chemistry*; John Wiley & Sons: New York, 1994; Vol. 42, pp 139−237. (b) Kanatzidis, M. G.; Sutorik, A. C. In *The Application of Polychalcogenide Salts to the Exploratory Synthesis of Solid State Multinary Chalcogenides at Intermediate Temperatures*; K. D. Karlin, Ed.; Progress in Inorganic Chemistry; John Wiley & Sons: New York, 1995; Vol. 43, pp 151−265.
(2) Savelsberg, G.; Schafer, H. *Z. Naturforsch* **1978**, *33B*, 711−13.
(3) Rudorff, W.: Schwarz, H. G.; Walter, M. *Z. Anorg. Allg. Chem.* **1952**, *269*, 141−52.
(4) Brown, D. B.; Zubieta, J. A.; Vella, P. A.; Wrobleski, J. T.; Watt, T.; Hatfield, W. E.; Day, P. *Inorg. Chem.* **1980**, *19*, 1945−50.
(5) Ghosh, B. P.; Chaudhury, M.; Nag, K. *J. Solid State Chem.* **1983**, *47*, 307−13.
(6) Vajenine, G. V.; Hoffmann, R. *Inorg. Chem.* **1996**, *35*, 451−57.
(7) Burschka, C. *Z. Naturforsch* **1979**, *34B*, 675−7.
(8) Burschka, C.; Bronger, W. *Z. Naturforsch.* **1977**, *32B*, 11−4.
(9) Ohtani, T.; Ogura, J.; Sakai, M.; Sano, Y. *Solid State Commun.* **1991**, *78*, 913−7.
(10) Ohtani, T.; Ogura, J.; Yoshihara, H.; Yokota, Y. *J. Solid State Chem.* **1995**, *115*, 379−89.

10.1021/cm980233d CCC: $15.00
Published on Web 08/29/1998

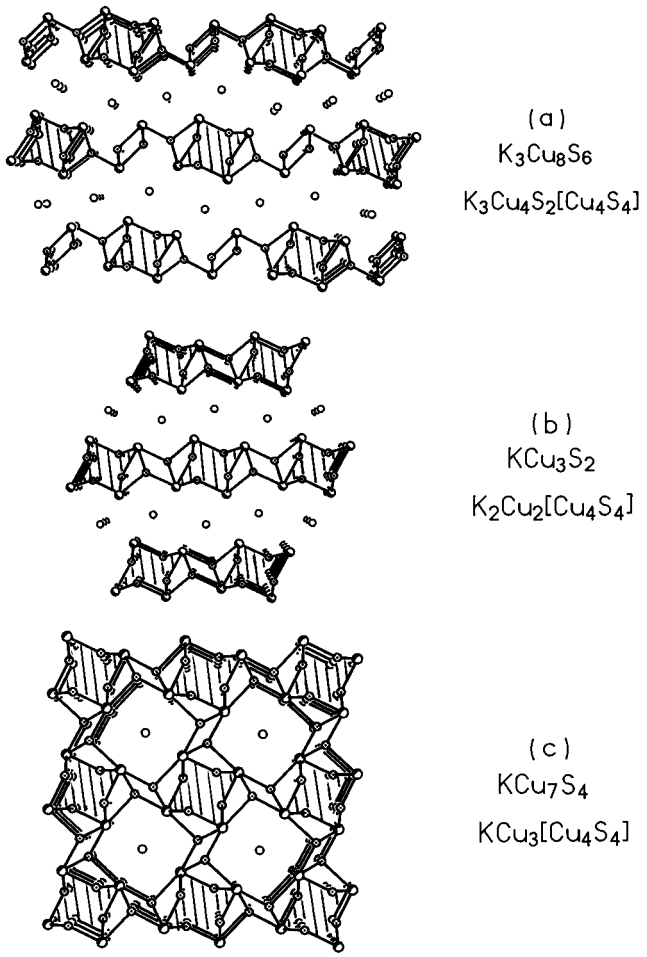

Figure 1. Structural similarity of (a) $K_3Cu_8S_6$, (b) KCu_3S_2, and (c) KCu_7S_4. Cu_4S_4 columns (shaded) are linked by copper chains to form Cu−S layers that are separated by K^+ cations in $K_3Cu_8S_6$ and KCu_3S_2. In KCu_7S_4, the K^+ cations reside in channels formed by the otherwise three-dimensional Cu−S network. The small dotted and open circles represent Cu and K, respectively, and the large shaded circles are S.

$[Cu_4S_4]$ ($\equiv 2 \times KCu_3S_2$), and $KCu_3[Cu_4S_4]$, respectively. (The Cu^+ cation outside the Cu_4S_4 column is four-coordinate.) In $K_3Cu_8S_6$ (Figure 1a), four copper and two sulfur atoms form parallel chains between adjacent columns. The columns and chains together form two-dimensional Cu_8S_6 ($\equiv Cu_4S_2[Cu_4S_4]$) layers, between which the K^+ cations reside. In KCu_3S_2 (Figure 1b), the distance between Cu_4S_4 columns is shortened because the adjacent columns are interlinked by chains of two copper atoms only. The KCu_7S_4 structure can be related to KCu_3S_2 first by aligning the adjacent $Cu_2[Cu_4S_4]$ layers in Figure 1b with respect to the columns and then by replacing half of the interlayer potassium with an additional pair of copper chains to form the channel structure in Figure 1c. The total occupancy of the 4-fold copper is 75% in order to form a chemically reasonable formulation, $(K^+)(Cu^+)_7(S^{2-})_4 \equiv KCu_3[Cu_4S_4]$.

The KCu_4S_3 and $K_3Cu_8S_6$ phases are mixed-valent, and the metallic conductivity arises from holes in the sulfur 3p band as the formal oxidation state of copper in copper chalcogenides is Cu^+.[11] This finding is of fundamental important for the understanding of the conducting mechanism of metallic chalcogenides.[4,12] The $K_3Cu_8S_6$ phase is thus far the most studied compound for its unusual low-temperature anomalies on transport properties.[13−18] Two phase transitions identified in $K_3Cu_8S_6$ are a second-order transition at 153 K and a first-order transition at 55 K accompanied by a sharp drop in resistivity. In earlier studies, researchers have considered the charge-density-wave (CDW) instability as being the origin of these transitions.

Ohtani et al. proposed that the so-called stoichiometric ACu_7S_4 (A = Tl, K, Rb) phases, like $K_3Cu_8S_6$, also exhibit CDW instability on the basis of the observed resistivity anomalies and supperlattice modulation from electron diffraction patterns.[9,10] Whangbo and Canadell later, however, argued that the electron-precise $ACu_7S_4 \equiv (A^+)(Cu^+)_7(S^{2-})_4$ cannot be a metal. For the as-grown sample to be metallic, they proposed that the true formula should be $A_{1-x}Cu_{3-y}(Cu_4S_4)$ ($x \neq 0$, $y \neq 0$).[18] The nonstoichiometry was indeed found in the synthetic *crookesite* ($TlCu_{7-x}Se_4$, $x = 0.5$).[19] Berger, et al. later further confirmed the nonstoichiometry in the isotypic $TlCu_{7-x}S_4$ ($0 \leq x < 0.55$) phase by neutron diffraction studies on powder samples.[20] We have recently established the nonstoichiometry range for the $KCu_{7-x}S_4$ ($0.00 \leq x \leq 0.34$)[21] and $RbCu_{7-x}S_4$ ($0.00 \leq x \leq 0.30$)[22] phases by X-ray diffraction studies of single-crystal samples. The stoichiometries for the samples prepared by Ohtani et al. are obtained as $TlCu_{6.85}S_4$,[20] $KCu_{6.87}S_4$, and $RbCu_{6.83}S_4$,[21,22] by interpolation of the cell volume vs copper content plots. Neither report has found vacancies that would give rise to nonstoichiometry on A-site cations. Through the electronic band structure calculations of $KCu_{7-x}S_4$[23] and temperature-dependent studies[24] of their resistance, thermal conductivity, thermoelectric power, and heat capacity (C_p) properties, we have come to the same conclusion as Berger et al.[20] that the resistivity anomalies likely originate from the ordering of Cu^+ cations. Accordingly, we have proposed a diffusive one-dimensional ordering model concerning the vacancy ordering of the chain-site copper cations at transitions.[24]

It is difficult to grow single crystals of ACu_7Q_4 (Q = S, Se) by conventional solid-state methods. Eriksson

(11) (a) Folmer, J. C. W.; Jellinek, F. *J. Less-Common Metals* **1980**, *76*, 153−62. (b) van Bruggen, C. F. *Ann Chim. (Paris)* **1982**, *7*, 171−203. (c) Rouxel, J. *Current Science* **1997**, *73*, 31−9.

(12) Hatfield, W. E., Ed. *Molecular Metals*; Plenum Press: New York, 1979.

(13) ter Haar, L. W.; DiSalvo, F. J.; Bair, H. E.; Fleming, R. M.; Waszczak, J. V.; Hatfield, W. E. *Phys. Rev. B* **1987**, *35*, 1932−8.

(14) Fleming, R. M.; ter Haar, L. W.; DiSalvo, F. J. *Phys. Rev. B* **1987**, *35*, 5388−91.

(15) Raghu, R.; Subramanyan, S. V.; Chatterjee, S. *Solid State Commun.* **1989**, *69*, 949−52.

(16) Sato, H.; Igaki, E.; Nakamura, T.; Ban, T.; Kojima, N. *Solid State Commun.* **1989**, *71*, 793−5.

(17) Sato, H.; Kojima, N.; Suzuki, K.; Enoki, T. *J. Phys. Soc. Jpn.* **1993**, *62*, 647−58.

(18) Whangbo, M.-H.; Canadell, E. *Solid State Commun.* **1992**, *81*, 895−9.

(19) Eriksson, L.; Werner, P.-E.; Berger, R.; Meerschaut, A. *J. Solid State Chem.* **1991**, *90*, 61−8.

(20) Berger, R.; Norén, L. *J. Alloys Comp.* **1996**, *237*, 33−8.

(21) Hwu, S.-J.; Li, H.; Mackay, R.; Kuo, Y.-K.; Skove, M. J.; Mahapatro, M.; Bucher, C. K.; Halladay, J. P.; Hayes, M. W. *Chem. Mater.* **1998**, *10*, 6−9.

(22) Li, H.; Hwu, S.-J. Unpublished research, Clemson University, 1997.

(23) Lee, K.-S.; Seo, D.-K.; Whangbo, M.-H.; Li, H.; Mackay, R.; Hwu, S.-J. *J. Solid State Chem.* **1997**, *134*, 5−9.

(24) Kuo, Y.-K.; Skove, M. J.; Verebelyi, D. T.; Li, H.; Mackay, R.; Hwu, S.-J.; Whangbo, M.-H.; Brill, J. W. *Phys. Rev. B* **1998**, *57*, 3315−25.

Table 1. Crystallographic Data for the $KCu_{7-x}S_4$ Series

	$KCu_{6.66(4)}S_4$ (**1a**)	$KCu_{6.69(5)}S_4$ (**1b**)	$KCu_{6.82(3)}S_4$ (**2a**)	$KCu_{6.88(5)}S_4$ (**2b**)	$KCu_{7.00(2)}S_4$ (**3a**)	$KCu_{7.00(2)}S_4$ (**3b**)
fw (amu)	590.7	592.6	601.0	604.5	612.5	612.5
space group	*I*4/*m* (No. 87)	*I*4/*m* (No. 87)	*I*4/*m* (No. 87)	*I*4/*m* (No. 87)	*P*4/*n* (No. 85)	*P*4/*n* (No. 85)
a , Å	10.179(2)	10.172(2)	10.177(2)	10.176(2)	10.177(2)	10.169(2)
c, Å	3.790(2)	3.791(2)	3.822(2)	3.834(2)	7.722(2)	7.708(2)
V, Å^3	392.7(2)	392.3(2)	395.8(2)	397.1(2)	799.8(3)	797.1(3)
Z	2	2	2	2	4	4
T, K	298	298	298	298	298	298
radiation	Mo Kα^d	Mo Kα^d	Mo Kα^d	Mo Kα^e	Mo Kα^e	Mo Kα^e
2θ range	3.5−60.0	3.5−50.0	3.5−50.0	3.5−55.0	3.0−55.0	3.0−55.0
ρ_{calc},[a] g cm^{-3}	4.996	5.017	5.042	5.056	5.086	5.105
abs coeff, cm^{-1}	191.98	192.97	194.68	195.50	197.38	198.13
R[b]	0.027	0.037	0.020	0.039	0.030	0.029
R_w[c]	0.031	0.037	0.021	0.049	0.038	0.037

[a] Calculated on the basis of the refined structural formula (see the text). [b] $R = \sum[|F_o| - |F_c|]/\sum|F_o|$. [c] $R_w = [\sum w[|F_o| - |F_c|]^2/\sum w|F_o|^2]^{1/2}$. [d] Rigaku AFC7R ($\lambda = 0.71073$ Å). [e] Refurbished Nicolet R3mV diffractometer ($\lambda = 0.71073$ Å).

et al. have proposed that the difficulty in obtaining good quality crystals is because of stacking fault in these copper-deficient phases.[19] Electrochemical (E-Chem) growth[25] is a convenient benchtop synthesis for the growth of large single crystals of the title series.[21] We can grow 1−2 cm long whiskers in a matter of 4 h. This enables us to carry out current studies based on single-crystal samples for the detailed investigations of once controversial issues concerning the nonstoichiometry and the space group.[9,19−20] Our results show that, at room temperature, the nonstoichiometric phases ($x > 0$) adopt the space group *I*4/*m* while the stoichiometric phase ($x = 0$) adopts *P*4/*n* with doubling in the *c*-axis. The former is consistent with the $TlCu_{7-x}S_4$ structure based on powder neutron diffraction.[20] Berger et al. also reported that the stoichiometric $TlCu_7S_4$ phase adopts the space group *I*4/*m*, and a phase transformation occurs at 255 K to the $CsAg_7S_4$ structure type[26] described as *P*4/*n*. Our temperature-dependent electron diffraction studies suggest that KCu_7S_4 possesses short-range order at room temperature (see the later discussion).

In this report we describe the single-crystal structures of the title series. In particular, we focus our attention on the room-temperature ordering patterns for the tetrahedral Cu^+ cations. We include some preliminary results from temperature-dependent magnetic susceptibility measurements and electron diffraction studies in an attempt to support our recently proposed diffusive one-dimensional ordering model.[24] We also briefly discuss the correlation in structure and properties with the previously studied $K_3Cu_8S_6$ phase.

Experimental Procedure

Synthesis. Crystals of $KCu_{7-x}S_4$ were grown in a two-electrode chemical cell. In a typical reaction, 1.0 g of K_2S (44%, the rest was other polysulfides, Alfa Æesar) and 0.5 g of CuCl (98+%, Aldrich) were loaded into a 100 mL round-bottom flask in a nitrogen-purged drybox. A rubber septum was used to cap the flask to protect the system from air, and a steady flow of dry nitrogen was maintained throughout the course of the reaction. A 50 mL portion of ethylenediamine (99%, Aldrich, dried over CaH_2 and distilled) was injected into the reaction flask. The resulting solution was preheated in a sand bath at 110 °C for 5 h to ensure that all of the electrolytes were dissolved. Two parallel electrode plates (1.5 × 1.5 cm^2; etched with the HNO_3 solution to remove the copper oxide layer) made from copper foil (0.254 mm thick; 99.9%, Alfa Æesar) were then immersed in the solution and connected to a constant voltage source. The applied voltage was typically between 0.5 and 3.5 V. The temperature of the E-Chem cell was controlled by a Gemini-2 Temperature Controller (J-KEM Scientific). Crystals of diffraction quality can be grown on the anode in about 1 h. The products were either washed with deionized water using the suction filtration method or dried on the Schlenk line.

Single-Crystal X-ray Diffraction. Six black needlelike crystals of $KCu_{7-x}S_4$ were mounted on glass fibers for single-crystal X-ray diffraction studies. Room-temperature crystallographic data are summarized in Table 1. Crystals **1a**, **1b**, and **2a** were thin, with typical dimensions of 0.03 × 0.03 × 0.50 mm^3. Data for these crystals were collected on a Rigaku AFC7R four-circle diffractometer emitting graphite-monochromated Mo Kα radiation ($\lambda = 0.71073$ Å) from a rotating anode. The other crystals, **2b**, **3a**, and **3b**, were larger, typically 0.05 × 0.05 × 0.75 mm^3, and data were collected on a Nicolet R3mV four-circle diffractometer, with graphite-monochromated Mo Kα radiation from a sealed tube anode.

The typical procedure for data collection can be described by that used for $KCu_{6.66(4)}S_4$, where $x = 0.34$. The unit cell parameters and orientation matrix for data collection were determined by a least-squares fit of 19 randomly located reflections in the range $11.4° < 2\theta < 19.8°$. Final unit cell parameters were determined from a least-squares fit of 24 high-angle reflections in the range $21.6° < 2\theta < 32.1°$. Data were collected using an $\omega-2\theta$ scan mode at 4°/min (with three or fewer rescans). A complete sphere of data was collected on the primitive triclinic cell ($2\theta_{max} = 50°$), resulting in a total of 1372 reflections, of which 192 unique reflections with $F > 6\sigma(F)$ were used for the final structure solution. There was no detectable decay during the data collection, according to the intensities of three standard reflections, which were measured every 100 reflections. Lorentz−polarization and empirical absorption corrections (ψ-scans) were applied to the data.[27] The structure was solved by direct methods with SHELXS-86[28] and refined on $|F|$ with SHELXTL-PLUS[29] by least-squares, full-matrix techniques.[30] Scattering factors for all atoms were taken from the source program used.

(25) For the knowledge of current development in nonaqueous electrochemistry, an excellent review on the electrochemical synthesis of telluride Zintl anions[a] and two recent reports on interesting main-group selenide anions[b, c] are cited as follows: (a) Warren, C. J.; Haushalter, R. C.; Bocarsly, A. B. *J. Alloys Compd*. **1995**, *229*, 175−205. (b) Park, C.-W.; Pell, M. A.; Ibers, J. A. *Inorg. Chem*. **1996**, *35*, 4555−8. (c) Pell, M. A.; Ibers, J. A. *Inorg. Chem*. **1996**, *35*, 4559−62.

(26) (a) Huster, J. *J. Alloys Compd*. **1992**, *183*, 377−84. (b) Wood, P. T.; Pennington, W. T.; Kolis, J. W. *Inorg. Chem*. **1994**, *33*, 1556−8.

(27) North, A. C. T.; Phillips, D. C.; Matthews, S. F. *Acta Crystallogr*. **1968**, *351*, 351−9.

(28) Sheldrick, G. M. In *Crystallographic Computing 3*; Sheldrick, G. M.; Krüger, C.; Goddard, R.; Eds.; Oxford University Press: London/New York, 1985; pp 175−89.

(29) Sheldrick, G. M. SHELXTL-PLUS, Version 4.2.1 Structure Determination Software Programs; Siemens Analytical X-ray Instruments Inc., Madison, WI, 1990.

(30) Busing, W. R.; Martin, K. O.; Levy, H. A. *ORFLS;* Report ORNL-TM-305; Oak Ridge National Laboratory, Oak Ridge, TN, 1962.

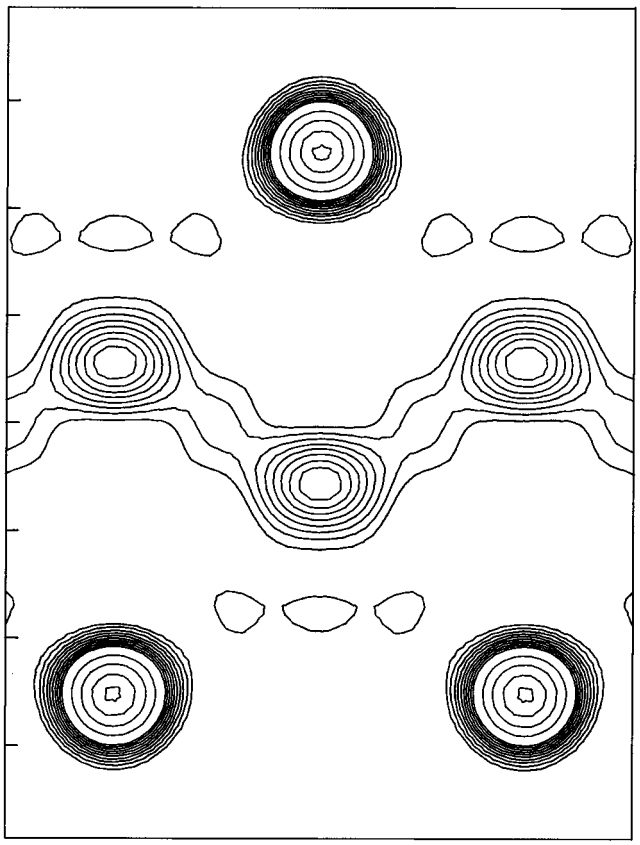

Figure 2. Fourier map of $KCu_{6.69(5)}S_4$ along the Cu(2)−Cu(3) chain. Contour levels are 1 $e^-/Å^3$.

A complete sphere of data was collected on the primitive triclinic cell to determine the correct space group and structure for this phase. Data reduction transformed the triclinic cell to the expected body-centered tetragonal unit cell. KCu_7S_4 has previously been reported to crystallize in $I\bar{4}$,[9,10] isostructural with $(NH_4)Cu_7S_4$,[31] both structure reports of which are based on powder diffraction data. As stated before, a recent report on an isostructural sulfide phase, $TlCu_7S_4$, from neutron diffraction data assigns the space group $I4/m$.[20] Additionally, the selenide analogue, from both single crystal [of the synthetic *crookesite*, $TlCu_{7-x}Se_4$ ($x = 0.5$)] and powder data,[19] is reported in the centrosymmetric space group $I4/m$. Extinction conditions for $I\bar{4}$ and $I4/m$ are identical. Intensity statistics on the KCu_7S_4 needle-shaped crystals suggested the centrosymmetric space group $I4/m$. The structure was successfully solved in this space group. The solution in the acentric $I\bar{4}$ was also tried, but it did not improve the refinement. Furthermore, the refinement result of the structure in $I\bar{4}$ was identical to its enantiomorph, again supporting the choice of the centrosymmetric solution as the correct structure. The same procedure of collecting a whole sphere of data was used for the sample with $x = 0.12$, and it gave similar results in the refinement. Only one or two octants of data were collected on the body-centered tetragonal cell of the other crystal structures with $x \neq 0$. The $x = 0$ phases were collected in a primitive tetragonal cell, with a doubled c-axis relative to the $x \neq 0$ phases. Axial photos along all axes showed consistent results.

We have carefully examined the occupancy of copper on the 4-fold sites. Fourier maps along the zigzag chain of the tetrahedral copper in the $KCu_{6.66(4)}S_4$ structure show the electron density smeared along the chain (Figure 2), suggesting that the copper atoms are partially displaced from the 4-fold sites. The Fourier map was calculated by refining the atomic parameters for K, S, and Cu in the Cu_4S_4 columns. No atoms were placed on the tetrahedral sites for this calculation to avoid biased results. A Cu atom, Cu(2), was placed on the tetrahedral site, and the positional and occupancy parameters were refined. The location of an additional Cu atom, Cu(3), was picked from the difference Fourier calculation and refined. The position, occupancy, and thermal displacement parameters of the disordered copper atoms were all allowed to be refined independently and simultaneously. The final refinement was carried out by allowing all atoms except Cu(3) to refine anisotropically. The thermal ellipsoids on Cu(2) became very large and anisotropic, but as the Fourier map shows, the electron density is distributed throughout the chain, and this model is sufficient to describe that disorder. A similar strategy was employed in the structure solution of all of these crystals, as all contained significant disorder. The positional and thermal parameters for three distinctive phases, **1a**, **2a**, and **3a**, are listed in Table 2. The selected bond distances and angles for **1a** are summarized in Table 3.

Table 2. Positional and Thermal Parameters[a] for the $KCu_{7-x}S_4$ Series

atom	x	y	z	B_{eq} (Å^2)	occupancy (%)
		$KCu_{6\ 66(4)}S_4$, **1a**			
K	0	0	0	1.66(8)	100
Cu(1)	0.0274(1)	0.3578(1)	0	1.97(8)	100
Cu(2)	0.3030(3)	0.2244(2)	0	4.18(8)	54.3(6)
Cu(3)	0.2695(8)	0.2434(9)	0.188(2)	1.2(2)	6.2(3)
S	0.2388(1)	0.4348(1)	0	1.18(8)	100
		$KCu_{6.82(3)}S_4$, **2a**			
K	0	0	0	1.50(8)	100
Cu(1)	0.0264(1)	0.3588(1)	0	1.89(8)	100
Cu(2)	0.3060(3)	0.2249(1)	0	4.11(8)	55.2(6)
Cu(3)	0.269(1)	0.245(1)	0.186(2)	1.3(2)	7.7(3)
S	0.2387(1)	0.4356(1)	0	1.03(8)	100
		$KCu_{7.00(2)}S_4$, **3a**			
K(1)	0.25	0.25	0.3763(4)	1.50(8)	100
K(2)	0.25	0.25	0.8773(3)	1.50(8)	100
Cu(1)	0.1132(1)	−0.2691(1)	0.1225(1)	1.74(8)	100
Cu(2)	0.2193(1)	−0.1068(1)	0.3780(1)	1.82(8)	100
Cu(3)	−0.0565(1)	0.0234(1)	0.3507(2)	3.16(8)	90.7(6)
Cu(4)	0.0	0.0	0.0	6.2(2)	82.1(7)
Cu(5)	−0.005(2)	−0.002(1)	0.261(2)	2.6(4)	7.5(5)
Cu(6)	0.065(1)	−0.024(1)	0.109(2)	3.2(3)	11.0(8)
S(1)	−0.0120(2)	0.1880(1)	0.1291(2)	1.03(8)	100
S(2)	0.0110(2)	−0.1873(1)	0.3748(2)	0.95(8)	100

[a] Equivalent iostropic thermal parameter defined as $B_{eq} = (8\pi^2/3)$ trace U.

Table 3. Selected Interatomic Distances (Å) and Angles (deg) for $KCu_{6.66(4)}S_4$

Cu(1)−S	2.290(2)	Cu(2)−S	2.239(2)
Cu(1)−S	2.334(1) × 2	Cu(2)−Cu(2)	2.242(3) × 2
Cu(1)−Cu(3)	2.596(8) × 2	Cu(2)−S	2.529(2) × 2
Cu(1)−Cu(2)	2.622(2)	Cu(2)−Cu(1)	2.622(2)
Cu(1)−Cu(2)	2.697(2) × 2	Cu(2)−S	2.673(3)
Cu(1)−Cu(3)	2.817(8) × 2	Cu(2)−Cu(1)	2.697(2) × 2
Cu(1)−Cu(1)	2.817(1) × 4	S−Cu(2)−S	97.1(1)
Cu(1)−Cu(1)	2.948(2)		101.7(1) × 2
Cu(1)−Cu(3)	2.985(9) × 2		103.8(1)
S−Cu(1)−S	108.6(1)		124.3(1) × 2
	121.6(1) × 2	Cu(3)−S	2.097(9)
S−Cu(3)	2.097(9) × 2	Cu(3)−S	2.168(9)
S−Cu(3)	2.168(9) × 2	Cu(3)−Cu(1)	2.596(8)
S−Cu(2)	2.239(2)	Cu(3)−Cu(1)	2.817(8)
S−Cu(1)	2.334(1) × 2	Cu(3)−Cu(1)	2.985(9)
S−Cu(2)	2.529(2) × 2	S−Cu(3)−S	163.0(5)
S−Cu(2)	2.673(3)	K−S	3.332(1) × 8
		K−Cu(1)	3.653(1) × 4

Powder X-ray Diffraction. The product identification was made by using powder X-ray diffraction methods. The room-temperature diffraction patterns were collected on a Scintag 2000 XDS $\theta-\theta$ diffractometer equipped with Cu Kα radiation ($\lambda = 1.5406$ Å). The powder patterns were taken from ground needle-shaped crystals, and the preferred orientation shown in the intensity profiles was inevitable. NIST

(31) von Gattow, G. *Acta Crystallogr.* **1957**, *10*, 549−53.

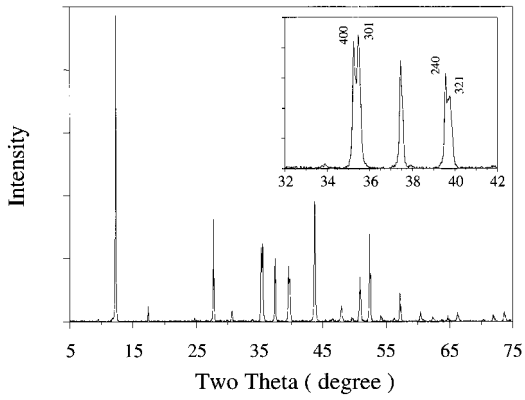

Figure 3. The powder X-ray diffraction patterns of $KCu_{6.66(4)}S_4$. The inset presents the typical peak splitting observed in the copper-deficient $KCu_{7-x}S_4$ phases.

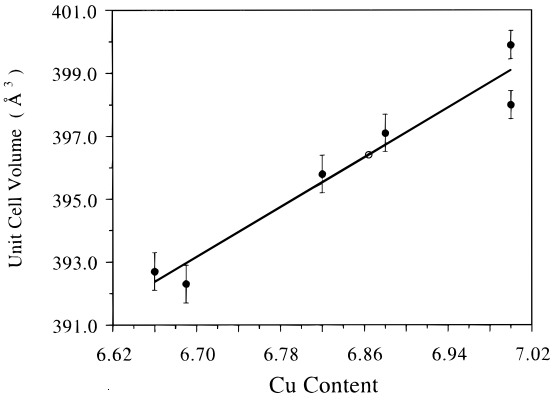

Figure 4. Normalized cell volume (solid circles) vs copper content plot for the $KCu_{7-x}S_4$ series. The error bars are drawn at $\pm 3\sigma$. A linear relation is shown by the straight line resulting from the least-squares fit of the data. The open circle represents the cell volume of the reported "KCu_7S_4" by Ohtani et al.; see the text.

(National Institute of Science and Technology) silicon powder was employed as an internal standard.

Figure 3 reports a typical set of powder X-ray diffraction patterns of the title series. For the crystals with lower copper content, a characteristic peak splitting (inset) occurs at $2\theta = \sim 35.4°$ (400 and 301) and $\sim 39.7°$ (240 and 321). This is attributed to the cell variation along the *c*-axis (Table 1). Superlattice reflections giving rise to doubling in *c* for the KCu_7S_4 phase, if present, are too weak to be observed. The unit cell volumes increase linearly with increasing copper content (Figure 4). The data points for the $x = 0$ phases are obtained by normalizing the cell volume since the true unit cell volume is doubled. From an interpolation of the plot, the phase reported by Ohtani et al.[10] has a copper content of $KCu_{6.86}S_4$.

Electrical Resistance and Thermoelectric Power Measurements. Electrical resistivity measurements were carried out for 4 K < *T* < 350 K using a conventional four-probe technique[32] on single crystals. Electrical contacts were made by first evaporating four indium pads on the sample, spaced along the longest dimension (*c*-axis) of the sample, and then applying silver paint. From the typical sample cross section of 50 μm × 5 μm and the distance between voltage contacts of 1 mm, it is estimated that the room-temperature resistivity along the needle axis is about 100 $\mu\Omega$ cm for the $x \neq 0$ phases and 10 mΩ cm for the stoichiometric $x = 0$ phase. This estimation can be off by at least a factor of 2, due to the uncertainty in the sample thickness.

(32) *Quick Reference Manual for Silicon Integrated Circuit Technology:* Beadle, W. E., Tsai, J. C. C., Plummer, R. D., Eds.; John Wiley and Sons: New York, 1985.

The temperature-dependent Seebeck coefficient *S* was measured on single crystals (along the *c*-direction, the needle axis) in the range 80 K < *T* < 300 K. For the sample mounting, one end of the crystal was connected to a controlled thermal bath with a fine silver wire. The other end was suspended freely in a vacuum and an electrical (and not-very-good thermal) contact was made to the other thermal bath. If the ends of the sample were both fixed to thermal bath, samples broke because of thermal contraction during the first cooling due to intrinsic brittleness. ΔT between the two thermal baths was 1−2 K throughout the measurements. Since ΔT between the thermal baths does not correspond to ΔT between the two ends of sample, our measurements of *S* are only qualitative. The sign and the qualitative temperature dependence of *S* are expected, nevertheless, to be valid. The measured *S* was not corrected for the contribution from the copper wire, so that the reported Seebeck coefficient is relative to that of copper.

Magnetic Measurements. The magnetic susceptibility was measured by using a Quantum Design SQUID MPMS-5S magnetometer. The measurements were carried out from 1.76 to 300 K in the field of $H = 0.5$ T. Powder sample (12.1 mg for **1a**, 10.2 mg for **2a**, 19.1 mg for **3a**) was contained in a gel capsule sample holder which was suspended in a straw from the sample translator drive. The temperature and field dependence of the susceptibility of the container were previously determined, and their effect was negligible. The magnetic susceptibility was also corrected for paramagnetic impurities as well as core diamagnetism.[33]

Electron Diffraction Studies. TEM (transmission electron microscopy) observations were carried out using an electron microscope (JEM-2000EX) with a double-tilt cooling holder (GATAN model 636) down to ~90 K. For recording the microscopic images and the diffraction patterns, an IP (imaging plate) system (Fuji FDL-5000) was used. The single crystals have a needlelike shape with dimensions ~0.02 mm × ~1.5 mm. The electron diffraction patterns were taken after the following procedures. The needle-shaped crystal was placed on a copper grid for the microscope (200 mesh) together with a drop of ethanol and then was broken into several fractions between two slide glasses.

Results

Synthesis. The compound formation depends on the concentration of electrolyte, choice of potassium polysulfide, and applied voltage. Experimental results from a set of selected reactions are summarized in Table 4, which lists results of our preliminary investigations on primary reaction conditions. The title series can be synthesized only with utilizing polysulfides, K_2S_n (n = 5, 6), not K_2S. This is because K_2S is not soluble in ethylenediamine. The original success using as-received "K_2S" was due to the polysulfide contaminants in the chemicals. We first used the commercial product "K_2S" (reactions 1−9), which contains up to 56% polysulfide impurities, according to the data sheet. We also notice that the as-received chemical contains an inconsistent amount of polysulfides and, consequently, we do not always get the $KCu_{7-x}S_4$ and/or KCu_5S_3[34] phases depending upon the content of the as-received chemical. This has prompted our later investigations (reactions 10−13) which suggest that only the soluble polysulfides, K_2S_n, can facilitate the phase formation. Since then, we have consistently grown the $KCu_{7-x}S_4$ crystals using

(33) O'Connor, C. J. *Prog. Inorg. Chem.* **1982**, *29*, 203−83.

(34) (a) The $K_xCu_5S_3$ ($x = 0.66$) phase was synthesized by using the as-received commercial product "K_2S". $K_xCu_5S_3$ crystallizes in the hexagonal space group $P6_3/mcm$ (No. 193) with $a = 7.0139(8)$ Å, $c = 7.266(2)$ Å, $V = 309.6(1)$ Å^3, and $Z = 2$ ($R = 0.047$, $R_w = 0.068$, GOF = 2.81). (b) Mahapatro, M. Bucher, C. K. Hwu, S.-J. Unpublished research, Rice University, 1994.

Table 4. Reaction Products of Selected Electrochemical Synthesis of the $KCu_{7-x}S_4$ Series

reaction no.	electrolytes	temp, °C	voltage, V	product[a]
1	K_2S_n[b]	110	0.5	ir
2			3.5	ir
3	2 K_2S_n[b]/CuCl	110	0.5	$KCu_{6.82(3)}S_4$[c]
4			3.4	$KCu_{6.69(5)}S_4$[c]
5	2 K_2S_n[b]/CuCl	110	0.0	KCu_4S_3[d]
6	2 K_2S_n[b]/CuCl	70	0.5	$KCu_{6.89(1)}S_4$[e]
7			1.0	$KCu_{6.78(1)}S_4$[e]
8	2 K_2S_n[b]/CuCl	40	1.0	unidentified phase
9	2 K_2S_n[b]/CuCl[f]	110	0.5	$KCu_{7.00(2)}S_4$[c]
10	K_2S[g]/CuCl	110	0.5	nr
11			3.0	nr
12	K_2S_5[g]	110	1.0	$KCu_{6.69(1)}S_4$[c]
13	K_2S_6[g]	110	1.0	$KCu_{6.98(1)}S_4$[c]
14	2 K_2S_5[g]/CuCl	110	1.0	$KCu_{6.93(1)}S_4$[c]
15	2 K_2S_6[g]/CuCl	110	0.5	$KCu_{6.82(1)}S_4$[c]
16			3.0	$KCu_{6.72(1)}S_4$[c]

[a] Anode product; ir, inconsistent result (see the text); nr, no reaction. [b] As-received K_2S (44%; the rest was other polysulfides). [c] Structural composition determined by SXRD. [d] Formed as precipitate including a trace amount of $KCu_{7-x}S_4$. [e] Poor crystal quality. [f] Trace amount of TiS_2 added for intended chemical doping. [g] Synthesized according to the procedures in ref 35.

polysulfides (reactions 12, 13) that are prepared in our laboratory following the reported procedures.[35] We also have had equal success using the K_2S_n/CuCl mixture (reactions 14, 15). The temperature studies (reactions 6−8) have shown that crystal growth occurs at as low as 70 °C. We have not observed growth of the title compounds at 40 °C but some unidentifiable needle phases on the anode in reaction 8. (The PXRD patterns are reported in Figure S1.) To grow the crystals of the $KCu_{7-x}S_4$ series, therefore, we need to keep the solution temperature above 70 °C but not to exceed the boiling point of ethylenediamine (116.5 °C). In terms of the copper content, we do see a close correlation between the nonstoichiometry and the applied voltage. Examining the conditions listed in Table 4, we observed that the higher the voltage, the lower the copper content. These results are reproducible, yielding phases with the desired copper contents. Without employing voltage (reaction 5), we have been able to produce crystalline products of KCu_4S_3, $KCu_{7-x}S_4$ (trace amount), and KCl from the metathesis reaction between K_2S_n and CuCl. With applied voltage, whiskers of the title compounds are grown on the anode in the direction perpendicular to the copper plate facing the cathode.

Although the detailed reaction mechanism is not understood, an approximate redox chemistry involving two half-cell reactions can be drawn: (1) anodic oxidation of copper $Cu \rightarrow Cu^+ + e^-$ and (2) cathodic reduction of polysulfide $S_n^{2-} + (2n - 2)e^- \rightarrow nS^{2-}$. This redox chemistry also explains why K_2S (reaction 5) does not yield the title compound. It is, presumably, because that the half reaction involving reduction of polysulfide, necessary for the complete cycle of the redox chemistry, does not exist in K_2S. The anodic dissolution is evident, with the copper electrode becoming much thinner at the end of reaction. Also, while the KCu_4S_3 phase is the major product of the metathesis reaction (reaction 5), according to the following chemical equation, the $KCu_{7-x}S_4$ phase is almost the exclusive phase from the E-Chem reaction.

$$19Cu + 3K_2S_5 + CuCl \rightarrow 5KCu_4S_3 + KCl$$

Structural Description. The controversy about the structure of $KCu_{7-x}S_4$ is resolved here by single-crystal X-ray diffraction methods. First, we have concluded that the space group for the body-centered tetragonal cell is $I4/m$ rather than $I\bar{4}$, again, in agreement with the reported structure of $TlCu_7S_4$[20] and $TlCu_7Se_4$.[19] This result likely applies to all other phases of this structure type, as suggested by Berger et al.[20] Second, the nonstoichiometry is attributed to the deficiency of copper. The literature reports the copper sites in the tetrahedral chain to be only 75% occupied in a random fashion. It has been suggested that the copper content is variable, but until recently there has been little evidence supporting this claim. Resistivity measurements of $TlCu_{7+x}S_4$, with $-0.05 < x < 0.10$, are reported as a function of temperature by Ohtani et al.[10] and show a compositional dependence, thus implying the existence of a range of homogeneity. The presence of excess copper, however, appears to be an incorrect conclusion. Spatially, one can imagine filling the vacant sites, as in $BaCu_8P_4$.[36] Chemically, however, increasing the copper content makes little sense. It would require a more reduced oxidation state of copper than Cu^+, suggestive of copper−copper bonding, which is not a plausible suggestion for this structure. On the basis of our results, the copper contents reported in the prior study are systematically too high (see below). The structure report on $TlCu_7Se_4$ also suggests deviation from the ideal stoichiometry, based on varying cell constants as well as refinement results, and systematic errors in their data prevented more conclusive results.[19] Recently, the stoichiometry of $TlCu_{7-x}S_4$ has been systematically varied by a copper extraction technique, removing copper all the way down to $TlCu_{6.45}S_4$.[20] The cell volume is found to vary linearly with copper content.

The results of the single-crystal X-ray diffraction experiments reported here show that this compound exists over a range of stoichiometry, so that $KCu_{7-x}S_4$ has a range in x at least as broad as $0.0 \leq x \leq 0.34$. When $x > 0$, the structure is best described as a body-centered tetragonal unit cell (Figure 1c). The copper content reported for each compound in Table 1 has been determined from refinement of the X-ray data. No independent quantitative elemental analysis has been performed on any of these samples, as no single measurement can conveniently accommodate the necessary 1% precision. The linear relationship between cell volume and copper content, as well as the distinctive transport properties measured, nevertheless provides sufficient accuracy for a determination of the relative copper content from cell volume alone, as seen in Figure 4. As mentioned above, the qualitative appearance of the powder X-ray diffraction patterns is very sensitive to the c/a ratio. The splitting or overlap of the 400/301 peaks and the 240/321 peaks is easy to notice, as they are all fairly strong peaks (Figure 3). In fact, this

(35) Brauer, G., Ed. *Handbook of Preparative Inorganic Chemistry*, 2nd ed.; Academic Press: New York, 1967.

(36) Pilchowski, I.; Mewis, A.; Wenzel, M.; Gruehn, R. *Z. Anorg. Allg. Chem.* **1990**, *588* 109−16.

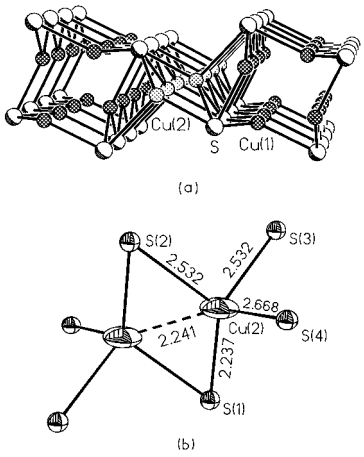

Figure 5. (a) Partial structure of the $KCu_{7-x}S_4$ phase viewed down along the needle axis. (b) Cu(2)−S and Cu(2)−Cu(2) distances associated with the Cu(2) atoms in the strongly distorted tetrahedral chains. The anisotropic thermal ellipsoids are drawn in 50% probability.

splitting was the first evidence of a significant range of stoichiometry, even before any single-crystal data were obtained.

As described in many reports, the extended structure of $KCu_{7-x}S_4$ consists of alternating Cu_4S_4 columns and tetrahedral Cu^+ cation chains interconnected to form pseudo-one-dimensional channels, where the K^+ cations reside. A general structure is shown in Figure 5a, where the partial structure of the framework is two parallel Cu_4S_4 columns interlinked by tetrahedral copper chains. It is immediately apparent that the coordination of copper cations is different: Cu(1) of the column is three-coordinate and Cu(2) of the chain is four-coordinate with respect to sulfur. From a close look at the bond distances, one realizes that $Cu(2)S_4$ forms a distorted tetrahedron (Figure 5b). The Cu(2)−S bond distances in the $KCu_{6.66}S_4$ structure (Table 3) are diverse, e.g., 2.24∼2.67 Å, while the Cu(1)−S bond lengths are more regular, e.g., 2.29∼2.33 Å, which are similar to those observed in Cu_2S (2.21−2.55 Å).[37] The tetrahedral distortion leaves space to allow the cation to rattle, as evidenced by the elongated thermal ellipses along the Cu(2)−S(3,4) direction. A similar distortion is seen in the $K_3Cu_8S_6$ strcuture,[7] and as pointed out by Whangbo and Canadell,[18] the resistivity anomalies are possibly due to the order−disorder transition of the tetrahedral copper. We do see sharp changes in resistivity (see later discussion) in the $x \neq 0$ samples whose structures possess distorted tetrahedral Cu(2) and residual copper cations in the chain.

The variable copper content is always associated with the disordered tetrahedral chain. The single crystal results show a complicated cation disordering that is beyond what has been reported. Besides the range of copper content, the extent of disorder of copper cation is phenomenal. Rather than a simple partial occupancy on the tetrahedral sites, Fourier maps show that significant electron density is located between the copper sites in the chain, indicating that copper atoms are also partially displaced from this site (Figure 6). When additional copper atoms are placed there in the

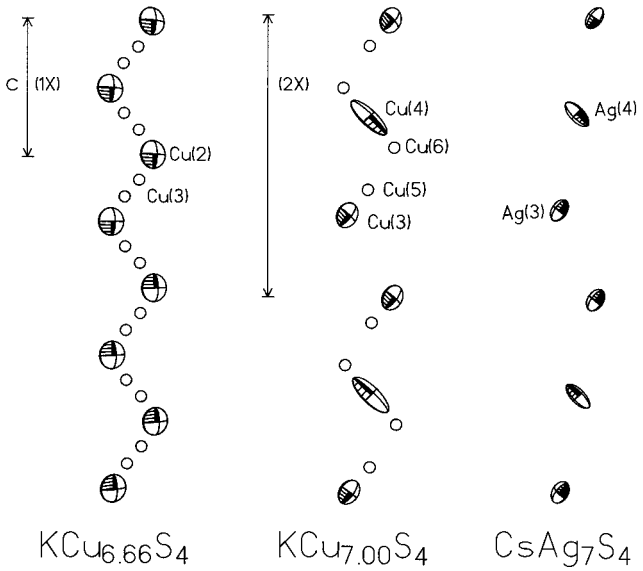

Figure 6. Disordered tetrahedral copper chain in the $KCu_{6.66}S_4$ and $KCu_{7.00}S_4$ phases and, for comparison, an analogous Ag chain in $CsAg_7S_4$[26] are plotted. The copper sites are partially occupied and the percent occupancies are refined; see the text. The disordering patterns of the $KCu_{6.88}S_4$ phase are similar to those of the $KCu_{6.66}S_4$ phase. The *c*-axis is doubled in $KCu_{7.00}S_4$, similar to that in the silver analogue. The anisotropic atoms are presented at 50% probability and the shaded octants and open circles represent major vs minor occupancy sites, respectively.

refinement, the occupancy of copper on the tetrahedral site decreases, and the sum of the occupancies on the two sites is always less than $(3 - x)/4$. The refined percent occupancies are 54.2(6)% and 6.2(6)% for Cu(2) (8h) and Cu(3) (16i) in **1a**, 55.2(6)% and 7.7(3)% for Cu(2) (8h) and Cu(3) (16I) in **2a**, and 91(1)%, 82(1)%, 7(1)%, and 11(2)% for Cu(3) (8g), Cu(4) (4d), Cu(5) (8g) and Cu(6) (8g) in **3a**, respectively.

The Cu−S distances and angles for the residual copper cations are normal. For $KCu_{6.66(4)}S_4$, for example, the Cu(3) atom has a nearly linear coordination to two sulfur atoms, with short Cu(3)−S distances of 2.07 and 2.19 Å and the S−Cu−S angle is 163.7°. These values are similar to those seen for two-coordinated copper in $NaCu_5S_3$ (d_{Cu-S} = 2.19 Å, and ∠(S−Cu−S) = 171.3°), which also has three-coordinate copper with d_{Cu-S} = 2.36 Å.[38]

The Cu−Cu interaction within the Cu_4S_4 column and between the column and the tetrahedral chain is weak judging from the longer distances than 2.56 Å found in elemental copper.[39] The Cu(1)−Cu(1) distances are 2.94 and 2.82 Å. The Cu(1)−Cu(2) distances of column and chain coppers are 2.62∼2.70 Å. The Cu(2)−Cu(2) distance along the zigzag tetrahedral chain, however, is 2.24 Å. This is the separation distance between two copper sites that are both occupied statistically, ca. 50%, and thus it is not an effective Cu−Cu distance, since the neighboring copper cations do not exist simultaneously.

A structural transformation is observed when the copper content is exactly $KCu_{7.00}S_4$. The superstructure

(37) Evans, H. T., Jr. *Nature (London), Phys. Sci.* **1971**, *232*, 69−70.

(38) Effenberger, H.; Pertlik, F. *Monats. für Chem.* **1985**, *116*, 921−6.

(39) Greenwood, N. N.; Earnshaw, A. *Chemistry of the Elements*; Pergamon Press: Oxford, U.K., 1984; pp 1366−1368.

observed has a doubled *c*-axis with a corresponding change in symmetry from $I4/m$ to $P4/n$. This phase transition may arise from a change in copper content, and the ordering observed here may suggest the type of ordering that occurs at low temperature. It is also likely that above room temperature this phase will undergo an order−disorder transition to the smaller, body-centered tetragonal cell, as observed for $TlCu_{7.00}S_4$ at 255 K.[20] The doubled unit cell results from ordering of tetrahedral copper, as well as a distortion of the chain. The structure is the same as that adopted by $RbAg_7S_4$ and $CsAg_7S_4$.[26] If we neglect the minor shifts in the Cu_4S_4 columns and consider only the copper chain, the nature of the transition is apparent in Figure 6. The copper-deficient structure, $KCu_{6.66}S_4$, for example, ideally contains a regular zigzag chain. The Cu arrangement in the $KCu_{7.00}S_4$ phase, instead of randomly occupying four sites with 75% occupancy, rearranges to completely occupy three sites. Compared to the structure of the $x > 0$ phases, the numbering of the metal atoms in $KCu_{7.00}S_4$ is changed. Cu(1) and Cu(2) correspond to the copper in the Cu_4S_4 columns, and Cu(3) and Cu(4) are the copper atoms in the chain. Cu(5) and Cu(6) are also in the chain, displaced from the ideal sites. Because of the rearrangement of the chain copper, the Cu(3)−Cu(4) gives a normal bond distance, 2.779(2) Å, comparable with those in the Cu_4S_4 column. In the Ag compounds, there is no indication of disorder along the Ag chain. In this copper compound, however, there is still significant disorder. Figure 6 shows some copper cations displacement off the tetrahedral site. Otherwise, the Cu(1)−S and Cu(2)−S distances fall within a narrow range, 2.27−2.35 Å. The Cu(3) atom is tetrahedrally coordinated, identical to the chain site in the copper-deficient samples. The Cu(3)−S distances are 2.26, 2.44, 2.62, and 2.74 Å. Cu(4) is linearly coordinated, with $d_{Cu(4)-S} = 2.16$ Å. The Cu(4) atom sits on an inversion center, and the S−Cu(4)−S angle is fixed at 180°. Interatomic distances for $KCu_{7.00(2)}S_4$ are in Table S3.

Although there is little change in the Cu−S distances and coordination in this superstructure, it is important to look at the change in the relative positions with regard to the copper network (Figure 7). In the $KCu_{7.00}S_4$ structure (Figure 7a), the copper atoms in the Cu_4S_4 column lie on the mirror planes perpendicular to the *c*-axis. Within a column, the copper atoms order along the *c*-axis in the fashion −Cu(1)−Cu(1)−Cu(2)−Cu(2)− to form the edge-shared Cu_4 tetrahedral copper core (hollow lines). The Cu(1)−Cu(1) distance in the *ab* plane is 2.81 Å, while the Cu(2)−Cu(2) distance is 2.98 Å. The vertical distance between the two adjacent Cu(1) layers is 2.74 Å, shorter than the distance between the adjacent Cu(2) layers, 2.83 Å. Between Cu(1)−Cu(2) layers, the distances also adopt a wide range from 2.79 to 2.90 Å. These distances, otherwise, are all comparable to the Cu(1)−Cu(1) distances, 2.82/2.92 and 2.82/2.95 Å, in the $x = 0.18$ and 0.34 phases, respectively (Figure 7b). Comparing these two structures in terms of the relative postions of the two structural units, one of the Cu^+ cations ion, Cu(4), in the tetrahedral chain of 7a is displaced along *z* to give rise to the doubled unit cell length. Consequentely, the Cu(4) atom lies between the two Cu(1) layers while the Cu(3) atoms of the chain remain on the same plane as Cu(2). In any case, the distortion in the column associated with the tetrahedral core is coupled with the doubling of the copper chain.

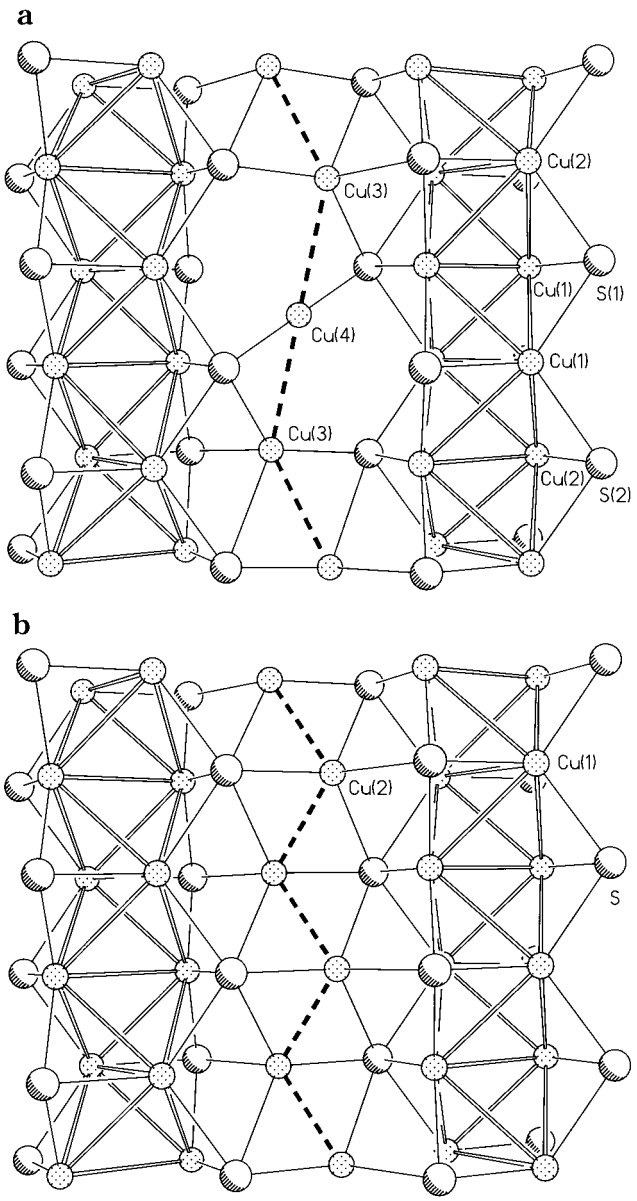

Figure 7. Partial structures of the $KCu_{7-x}S_4$ series, (a) $x = 0.0$ and (b) $x > 0$, showing two Cu_4S_4 columns (with the copper core outlined in hollow lines) and tetrahedral chains (dashed lines).

Electrical Conductivity and Thermoelectric Power. Resistivity measurements on single-crystal samples show a strong dependence on copper content and exhibit significant hystereses at the transitions, especially for the $x = 0.0$ and 0.12 samples (Figure 8). It is noticed that the room-temperature resistivity along the *c* axis, 100 $\mu\Omega$ cm, for the $x > 0$ phases, is about the same order of magnitude as that of $K_3Cu_8S_6$,[17] and is 100 times smaller than 10 mΩ cm for the $x = 0$ phase.[24] Samples of $KCu_{7.00}S_4$ show semiconducting behavior throughout the temperature range of 10∼300 K. There is a jump in resistivity observed slightly below 300 K. Semiconducting behavior is expected with this stoichiometry, when all energy bands are filled.[23] With decreasing copper content the sulfur is oxidized, creating holes in the sulfur 3p band. At $x = 0.34$, the material

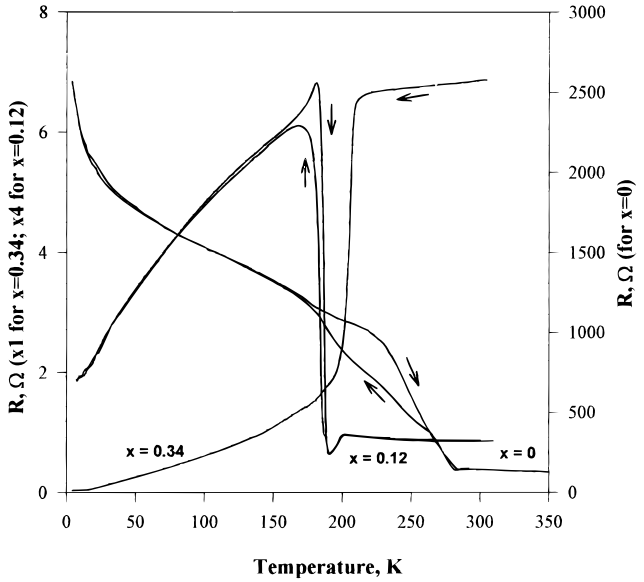

Figure 8. Temperature-dependent resistance (R) of the single-crystal samples of the $KCu_{7-x}S_4$ (x = 0.0, 0.12, 0.34) series. R is hysteretic between 180 and 280 K, for x = 0.0, and between 150 and 190 K, for x = 0.12. The x = 0.34 sample exhibits little hysteresis, which is not shown for clarity. It is estimated that the room-temperature resistivity along the needle axis is about 100 $\mu\Omega$ cm for the $x \neq 0$ phases, and 10 mΩ cm for the stoichiometric x = 0 phase.

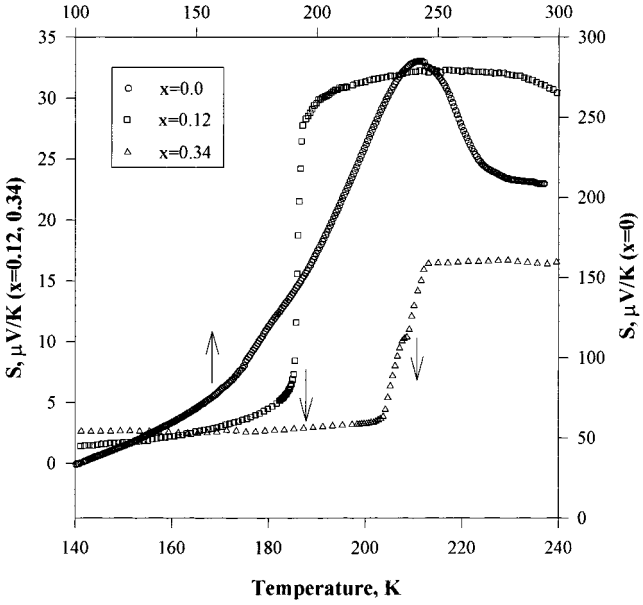

Figure 9. Temperature-dependent thermoelectric power of the single crystals of the $KCu_{7-x}S_4$ (x = 0.0, 0.12, 0.34) series near their transitions. All data were taken on warming. The values of S are relative to that of copper (ref 24).

exhibits metallic behavior throughout the entire temperature range, with an abrupt drop at ~208 K. As the temperature decreases, the x = 0.12 material displays a semimetal-to-metal transition at ~185 K, similar to what has been reported by Ohtani et al.[10] This result, in addition to the reported cell volume, again supports the claim that the material used in the previous investigation was, instead of KCu_7S_4, deficient in copper composition. Comparing the resistivity of single-crystal samples and pressed pellets confirms the anisotropy expected in this material.[21]

The thermoelectric power measurements (Figure 9) show that the Seebeck coefficients S for the x = 0 samples are much larger than that of the samples with $x > 0$ and have a temperature dependence similar to that found for R. For the x = 0.34 sample, an obvious kink is shown at 208 K, which is not observed in the R curve. In all cases, the values of S are positive, which implies that the carriers are holes. For the x = 0.12 sample, the changes in S and R around the transitions have opposite signs, which is unusual. In the report by Ohtani et al., however, the sign of S changes from positive to negative at ~175 K on the basis of pressed-pellet samples.

Magnetic Susceptibility. The magnetic susceptibility (χ) of ground single-crystal samples show mostly temperature-independent Pauli paramagnetism (Figure 10). The data were first corrected for the core diamagnetism and then fitted with the equation $\chi = \chi_o + C/T$ for the Curie constant (C) from the χ vs $1/T$ plot. The Curie tail shown at low temperature in the original data is likely due to impurities such as those that might come from the copper electrode. The Curie constants are 4.22×10^{-3}, 1.86×10^{-2}, and 1.44×10^{-2} emu K mol^{-1} for the x = 0.0, 0.12, 0.34 phases, respectively. For the x = 0.00 curve, the enlarged figure (not shown) indicates correlation with the aforementioned phase transitions,

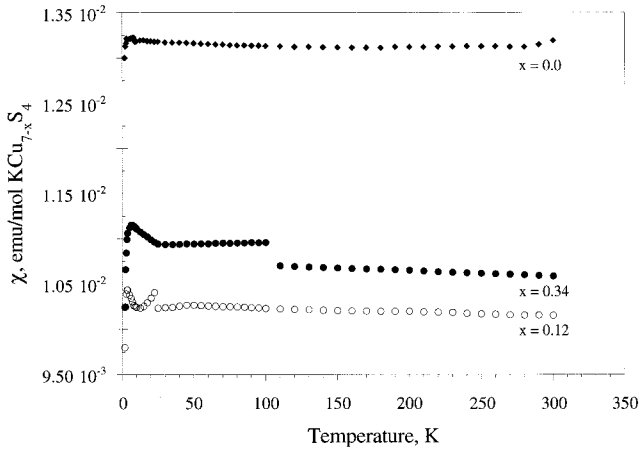

Figure 10. Magnetic susceptibility of the $KCu_{7-x}S_4$ (x = 0.0, 0.12, 0.34) series. The abrupt jumps at ca. 100 K for the x = 0.34 phase and at ca. 20 K for the x = 0.12 phase are likely due to instrumental error.

but the magnitude of $\Delta\chi$ at these transitions is very small, except for the one at ca. 280 K (Figure 10), which matches with the transition observed in the R vs T plot. The jump at ~100 K for the x = 0.34 curve is likely due to the instrumentation. It is apparent that the resistivity changes are not associated with large x changes. This may mean that the changes in resistivity are due to mean free path effects due to ordering. Detailed magnetic susceptibility analysis is underway. The present magnetic measurements show little correlation, if at all, with the previously studied "KCu_7S_4". We also notice that the $KCu_{7.00}S_4$ sample does not show diamagnetic response, as it should be if it is an electron-precise compound, but a Pauli paramagnetism. We speculate that the sample may be contaminated by copper-deficient compounds. A systematic investigation of magnetic properties and microprobe analysis necessary for the correlation studies are in order.

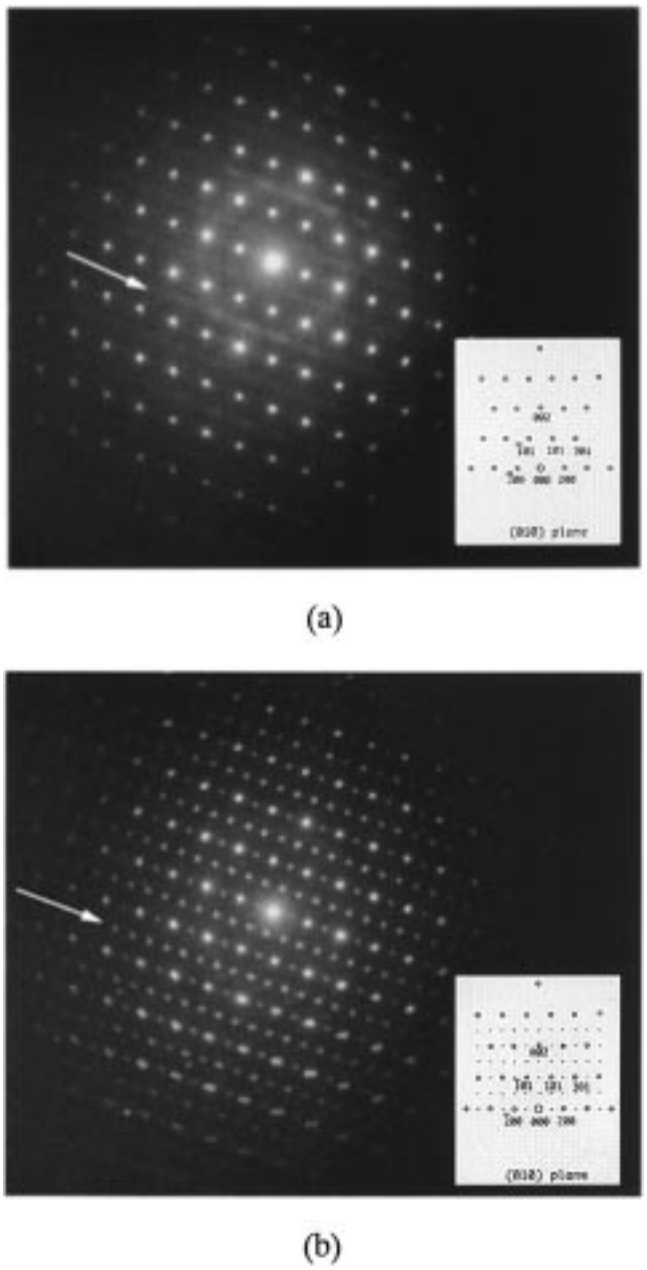

Figure 11. Electron diffraction patterns of the $KCu_{7.00}S_4$ phase. The streaks seen in (a) the room-temperature pattern, top, eventually become distinct spots in (b) the low-temperature (100 K) pattern, bottom. The indices are shown in the inset; see the text.

Electron Diffraction. Figure 11 shows electron diffraction patterns for a $KCu_{7.00}S_4$ sample. The incident beam is perpendicular to the (010) plane. Note that the (h00) and (00l) spots are observed when $h = 2n$ and $l = 2n$, inconsistent with $P4/n$. Particularly interesting are the streaks in the pattern taken at 35 °C (see arrow in Figure 11a), which indicate that short-range order is already present well above the ~280 K transition. Figure 11b, taken at 100 K, shows that the incipient order present at 35 °C becomes long-range order below the transition. The superlattice spots appear in the c^*-direction with $q = c^*/2$, as in previous work.[10] We also note that the 35 °C streaks are more clearly observed in patterns that are taken after warming from 100 K than they are in patterns taken before cooling, with superlattice spots beginning to appear in the streak line in the patterns taken after warming. This is consistent with the hysteresis seen in the resistance and heat capacity and implies that the ordering process may involve diffusion.

Discussion

Although the Fourier map in Figure 2 is reminiscent of that seen in some ionic conductors, this refinement is discussed in terms of a static disorder, not ionic conductivity. No impedance measurements have been carried out to measure the ionic conductivity of this material, but as has been pointed out, the resistivity trend previously reported does not support the presence of ionic conductivity below room temperature nor is any frequency dependence of the conductivity observed.[18]

The preferential formation of $KCu_{7-x}S_4$ in this electrochemical cell may arise from kinetic factors. This is the most copper-rich phase in the ternary K−Cu−S system. Its formation is not a function of concentration of K_2S_n or CuCl, as reactions have been done in which the concentration has been varied by a factor of over 40. The local high concentration of Cu ions around the anode in these unstirred electrochemical cells may favor the formation of the $KCu_{7-x}S_4$ phase.

The Cu_4S_4 columns and connecting Cu chains are a common feature in the $K_3Cu_8S_6$, KCu_3S_2, and KCu_7S_4 structures. The Cu−P network in $BaCu_8P_4$ is similar to the Cu−S network in KCu_7S_4, except all the copper chain sites are filled.[36] In each of these compounds, except KCu_7S_4, the chain sites are fully occupied, and there is no report of disorder. The single-crystal refinement of $K_3Cu_8S_6$,[7] however, shows large thermal parameters for copper atoms on the chain site, as stated before, which may suggest some copper deficiency or disorder. In contrast, the refinement of the copper parameters in $BaCu_8P_4$ seems well-behaved. Apparently, the bonding within the Cu−S network is sufficiently strong that it can accommodate a large deficiency of copper in the chains and retain its overall structural integrity, as observed in $KCu_{7-x}S_4$. It appears to accommodate deficiencies in two distinct ways: by random vacancies, when $x > 0$, and by distortion of the chain, when $x = 0$. The X-ray diffraction data has been interpreted as showing the formation of random vacancies along the chain. A model concerning the formation of regions of local ordering should not be ruled out. In other words, even in copper-deficient phases, the ordering of vacancies is not necessarily totally random.

The distortion which occurs with the stoichiometric $KCu_{7.00}S_4$ phase can be rationalized by condsidering site preferences. Pauling bond order, an empirical calculation which scales as bond strengths,[40] suggests a site preference for the two-coordinate copper site over that of either the three-coordinate site in the column or the four-coordinate copper site in the chain. This could be a sufficient driving force for the distortion. Vacancies on the zigzag chain remove the steric hindrance for this distortion.

The ordering of the chain for the stoichiometric phase does not explain the disorder and apparent random

(40) Pauling, L. *The Nature of the Chemical Bond*, 3rd ed.; Cornell University Press: Ithaca, 1960.

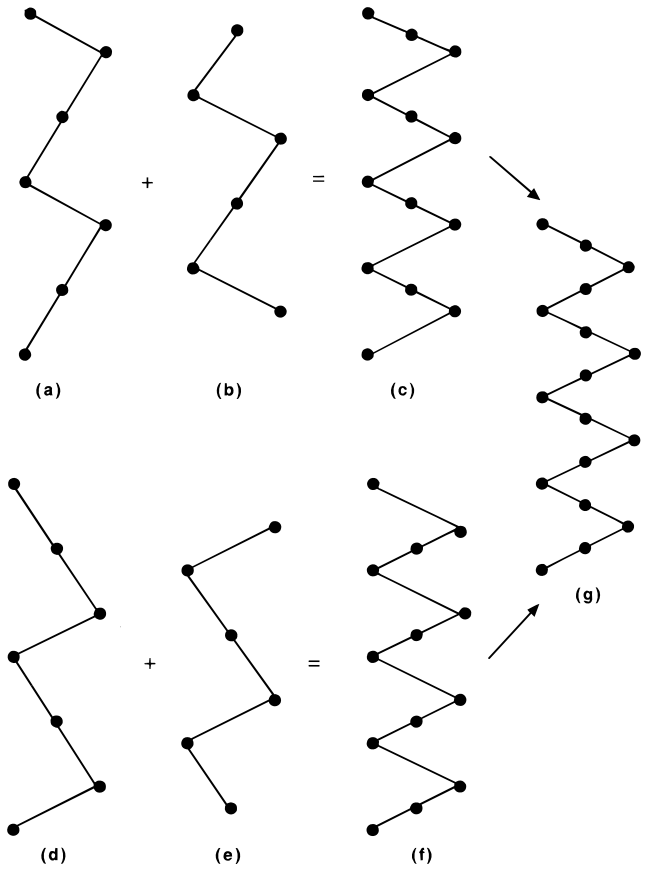

Figure 12. One model by which local ordering along the copper deficient chains could give the appearance of a disordered chain; see the text.

vacancies observed in the copper-deficient samples. One possibility not previously discussed is the idea of local ordering in the overall disordered model. These can be in either of two perpendicular directions, *a* and *b*, and if blocks or regions form with alternating orientation in a single crystal, the mixing is averaged in the single-crystal solution, resulting in tetragonal symmetry.

A second model for the disorder is based on the ordering observed in the doubled unit cell with $x = 0$ (Figure 6). A short fragment of the chain is shown in Figure 12a. If the fragment is displaced by one-half its repeat distance, it will look like the fragment in Figure 12b. When the two fragments are overlapped, the resultant chain is illustrated in Figure 12c. Note that the repeat distance is half the repeat distance of the ordered chain fragment. Each fragment contains fully occupied copper sites with the vacancies occurring between fragments. The vacancies cause a disruption of the fragment and a displacement relative to the initial repeat unit. The averaged cell consists of a disordered zigzag chain. Consider now the location of the chain with respect to the $\bar{4}$ axis in the unit cell. If one chain is ordered as in Figure 12a, the effect of the $\bar{4}$ axis is to make an adjacent chain ordered, as in Figure 12d. As before, the displacement, (Figure 12e) and overlapping (Figure 12f) of the chains results in an averaged structure with a repeat distance half that of the original. As all of these types of ordering are possible within a single chain, the complete combination of these two patterns results in the final chain shown in Figure 12g. This is almost exactly the result observed in the single-crystal diffraction experiments: a zigzag chain with copper sites located between the corner sites. In the actual refinements the copper is displaced from the midpoint positions depicted in this model. Furthermore, each corner site in this model has a contribution from two of the four individual models (a, b, d, e) or has a statistical 50% occupancy. The linear sites are each unique to one of the four models, so these sites are statistically 25% occupied. (In the actual refinements, this site was off the inversion center and thus split into two sites, where each split site would ideally be 12.5% filled.) It is fascinating to see that the actual refinement results indicate a matching occupancy of the corner sites of 55% and the other site with variable occupancy from 6 to 10% (depending on copper concentration). Again, the mixing of fragments of an ordered chain is possible with vacancies which occur between the chain fragments.

If the crystal truly contains this second type of disorder, one might consider the effect that this will have on the rest of the structure. In $KCu_{7-x}S_4$, with a short *c*-axis, all copper atoms in the Cu_4S_4 columns are crystallographically identical. In the $KCu_{7.00}S_4$ phase, with a doubled *c*-axis, they are split into two crystallographic sites. The two sites are separated from each other by 1/2 in *z*. In Table 2, if the projected (*x*,*y*) positions of the Cu(1) atom ≡ Cu(1)′ , (−0.23, 0.11), and the Cu(2) ≡ Cu(2)′, (0.28, 0.61), are averaged, the new position is equal to the observed (0.03, 0.36) of Cu(1) in the $KCu_{6.82}S_4$ phase. The averaging of sulfur positions gives similar results. In other words, if the structure of the copper-deficient phases is actually made of segments of the ordered stoichiometric phase, the observed structure is a result of the overlapping and averaging of the "ideal" structure. Although this does not prove local ordering, it provides a self-consistent model for the disorder, based on local ordering rather than random site occupancy.

In fact, both the low-temperature X-ray diffraction[41] and electron diffraction results on single-crystal samples are consistent with the hypothesis of having "composite" diffraction patterns due to local ordering. Attempts to index the single crystals of the title series failed at temperatures below the transitions. The peak profiles were split at low temperatures, resulting in unindexable patterns. As the crystal warmed back up to the room temperature, however, it can be reindexed just as it was before. Our Rietveld profile analysis showed that the $x > 0$ materials undergo a tetragonal to monoclinic phase transition between 185 and 195 K, while the $x = 0$ compound does not exhibit phase changes.[41] The electron diffraction patterns showed large sample dependence. The preliminary results on the $x = 0.34$ sample showed that the superstructure has the vector $q = 1/3a^* - 2/3b^* + 1/3c^*$.

Other supercells can also be described by retaining local order. For instance, the tripled unit cell suggested with lower copper content ($x > 0$), or associated with a low-temperature phase transition, might be modeled by a chain such as the one below (I−III). Models with local ordering avoid clustering of vacancies, for which there is no apparent driving force.

(41) Mackay, R.; Li, H.; Hwu, S.-J. Unpublished results, 1997.

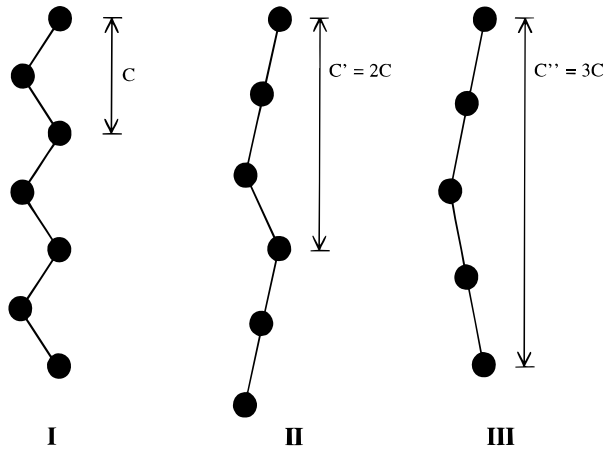

Concluding Remarks

The present investigations have shown that the KCu_7S_4 series exhibits complicated structural patterns, and much more work in temperature-dependent studies needs to be done to reveal the origin of phases transitions identified by transport property measurements. The single crystal studies suggest that the nonstoichiometry with respect to the copper content is extended from the already partially occupied tetrahedral Cu^+ cation chain. We believe the "KCu_7S_4" previously studied by Ohtani et al.[10] to be copper-deficient and that the real composition, based on the interpolated cell volume and matched transport properties, is $KCu_{6.86}S_4$. The ordering of Cu^+ cations gives rise to superstructures and different space groups. The $KCu_{7-x}S_4$ series adopts two space groups, $I4/m$ (instead of $I\bar{4}$) for $x > 0$ phases and $P4/n$ for the $x = 0$ phase. Preliminary temperature-dependent electron diffraction studies show, however, that the room-temperature (or slightly above room temperature) structure of the $x = 0$ phase may also crystallize in the space group $I4/m$. At room-temperature we see a faint line, consistent with doubling of the lattice along the *c*-axis, which becomes a row of distinct spots at low temperature. It is also interesting that a small variation of copper concentration changes the transport properties significantly. The $KCu_{7-x}S_4$ samples with different copper concentrations ($x = 0.0, 0.12, 0.34$) not only show unique successive transitions in the R vs T plots but also exhibit significant hysteresis at the transitions. The abrupt transition at ca. 208 K seen in the most copper-deficient phase, $x = 0.34$, is also seen in the $K_3Cu_8S_6$ sample, but at a much lowered temperature. While those anomalies in the resistivity measurements were proposed to be CDW-like transitions, there is new evidence showing they can be interpreted as order−disorder, cation diffusive transitions. In any event, it is clear that systematic studies on temperature-dependent properties are in order. We have demonstrated that crystals grown by electrochemical methods possess superior properties in their controlled stoichiometry, size, and quantity. Finally, the materials can be prepared conveniently and precisely in only a brief span of time. This facilitates a steady sample source for an in-depth study of structure/property correlation.

Acknowledgment. We thank Dr. M. Whangbo, Dr. W. T. Pennington, and Dr. G. L. Schimek for helpful discussions. Acknowledgment is made to the donors of the Petroleum Research Fund, administered by the American Chemical Society (S.J.H.), and to the Office of Energy Research, Basic Energy Sciences, Materials Science Division, U.S. Department of Energy (M.J.S.), for support of this research.

Supporting Information Available: Tables of detailed crystallographic data for the $KCu_{7-x}S_4$ series, positional and thermal parameters, and selected bond distances and angles (13 pages); observed and calculated structure factors (8 pages). Ordering information is given on any current masthead page.

CM980233D